Development 140, 2130-2138 (2013) doi:10.1242/dev.089409

Decoupling the function of Hox and Shh in developing limb reveals multiple inputs of Hox genes on limb growth

Rushikesh Sheth[1], Damien Grégoire[1,*], Annie Dumouchel[1], Martina Scotti[1], Jessica My Trang Pham[1], Stephen Nemec[2], Maria Félix Bastida[3], Marian A. Ros[3,‡] and Marie Kmita[1,4,‡]

SUMMARY

Limb development relies on an exquisite coordination between growth and patterning, but the underlying mechanisms remain elusive. Anterior-posterior and proximal-distal specification initiates in early limb bud concomitantly with the proliferative expansion of limb cells. Previous studies have shown that limb bud growth initially relies on fibroblast growth factors (FGFs) produced in the apical ectodermal ridge (AER-FGFs), the maintenance of which relies on a positive-feedback loop involving sonic hedgehog (Shh) and the BMP antagonist gremlin 1 (Grem1). The positive cross-regulation between *Shh* and the HoxA and HoxD clustered genes identified an indirect effect of Hox genes on the maintenance of AER-FGFs but the respective function of *Shh* and Hox genes in this process remains unknown. Here, by uncoupling Hox and *Shh* function, we show that HoxA and HoxD genes are required for proper AER-FGFs expression, independently of their function in controlling *Shh* expression. In addition, we provide evidence that the Hox-dependent control of AER-FGF expression is achieved through the regulation of key mesenchymal signals, namely *Grem1* and *Fgf10*, ensuring proper epithelial-mesenchymal interactions. Notably, HoxA and HoxD genes contribute to both the initial activation of *Grem1* and the subsequent anterior expansion of its expression domain. We propose that the intricate interactions between Hox genes and the FGF and Shh signaling pathways act as a molecular network that ensures proper limb bud growth and patterning, probably contributing to the coordination of these two processes.

KEY WORDS: FGF, Gremlin 1, Hox genes, Shh, Limb development, Organ growth, Mouse

INTRODUCTION

One of the most intriguing issues in developmental biology is how organ growth and patterning are coordinated during embryogenesis. For example, in vertebrates, the formation of the main body plan is achieved through posterior elongation, and cells ingressing through the primitive streak progressively express more posterior identity genes. Similarly, limb development relies on an exquisite coordination between growth and patterning, but the underlying mechanisms remain elusive. Limb outgrowth requires FGF signaling from the AER (Fallon et al., 1994; Niswander and Martin, 1993), provided by *Fgf4*, *Fgf8*, *Fgf9* and *Fgf17* (collectively called AER-FGFs). Among them, *Fgf8* is the only FGF expressed from nascent AER until AER regression and is sufficient to ensure virtually normal limb development in absence of the other AER-FGFs (Boulet et al., 2004; Moon et al., 2000; Sun et al., 2000; Sun et al., 2002). Three mesenchymal factors, *Fgf10*, *Shh* and the BMP antagonist *Grem1* are essential for correct expression of AER-FGFs (Laufer et al., 1994; Ohuchi et al., 1997; Zúñiga et al., 1999). Initially, in the presumptive limb field of the lateral plate mesoderm (LPM), *Fgf10* triggers the expression of *Fgf8* in the overlaying ectoderm, which in turn maintains *Fgf10* expression in the early limb bud (Ohuchi et al., 1997). Subsequently, further growth along the proximodistal (PD) axis and the anteroposterior (AP) expansion of the distal bud (presumptive hand/foot) is driven by a positive regulatory feedback loop between Shh, Grem1 and AER-FGFs, with Shh signaling being required to maintain *Grem1* transcription while the latter preserves expression of AER-FGFs by antagonizing BMPs (e.g. Zeller et al., 2009). In mice, expression of *Shh* and AER-FGFs regresses around E13 and subsequent growth of the limb relies on the elongation of skeletal elements.

The combined inactivation of the HoxA and HoxD gene clusters previously revealed their requirement for the activation and maintenance of *Shh* expression (Kmita et al., 2005). These genes are members of the Hox family, which encode transcription factors that control patterning events during embryogenesis. In most vertebrates, Hox genes are grouped into four clusters (HoxA to HoxD) in which the relative order of the genes on the chromosome parallels their serial expression in time and space, a phenomenon referred to as temporal and spatial co-linearity (Duboule and Morata, 1994). For example, in nascent limb buds, genes from the HoxA and HoxD clusters are activated sequentially in time (from group 1 to group 13) and their expression patterns switch from uniform for early activated genes to posteriorly restricted for later activated ones (reviewed by Zakany and Duboule, 2007). Interestingly, only those expressed in the posterior limb mesenchyme (group 10 to 13) are able to activate *Shh in vivo* (Tarchini et al., 2006) via direct activation of the *Shh* limb enhancer (Capellini et al., 2006), thereby establishing a link between the co-linear Hox activation and *Shh*-dependent AP polarity (Tarchini et al., 2006). Accordingly, ectopic/precocious expression of *Hoxd13* and *Hoxd12* anteriorly results in mirror-image expression of *Shh* and bilaterally symmetrical limbs (Knezevic et al., 1997; Zákány et al., 2004). Recent studies showed that the activation of *Shh* actually relies on a Hox-Hand2 protein complex (Galli et al., 2010) and

[1]Laboratory of Genetics and Development, Institut de Recherches Cliniques de Montréal (IRCM), 110 avenue des Pins Ouest, H2W1R7, Montréal, Québec, Canada. [2]Laboratory of Molecular Genetics, Institut de Recherches Cliniques de Montréal (IRCM), 110 avenue des Pins Ouest, H2W1R7, Montréal, Québec, Canada. [3]Instituto de Biomedicina y Biotecnología de Cantabria, CSIC-University of Cantabria-SODERCAN, Herrera Oria s/n, 39011 Santander, Spain. [4]Department of Medicine, Université de Montréal, Montréal, Québec, Canada.

*Present address: Institut de Génétique Moléculaire de Montpellier, CNRS UMR5535, 1919 route de Mende, 34293 Montpellier, France
‡Authors for correspondence (rosm@unican.es; marie.kmita@ircm.qc.ca)

Accepted 15 March 2013

Hand2 itself is activated by paralogous group 9 Hox genes (Xu and Wellik, 2011). Together, these results show both direct and indirect control of *Shh* expression by specific members of the Hox family of transcription factors. In turn, Shh signaling is required for the maintenance of HoxA and HoxD gene expression by inhibiting the proteolytic cleavage of the Gli3 protein into a transcriptional repressor (Litingtung et al., 2002; te Welscher et al., 2002).

Inactivation of the HoxA and HoxD clusters eventually results in severe reduction of the limb size, which was initially associated with *Shh* downregulation (Kmita et al., 2005). However, the respective role of *Shh* and HoxA;D genes has remained unclear owing to the Hox-Shh positive cross-regulation. In addition, $Shh^{-/-}$ limb shortening is significantly less severe compared with the double *HoxA;HoxD* mutant (Chiang et al., 2001; Kmita et al., 2005; Kraus et al., 2001) suggesting that HoxA and HoxD genes also impact on limb growth independently of their control of *Shh* expression. Here, we report on the Hox-dependent limb growth in contexts where Hox and *Shh* functions are uncoupled. First, by investigating HoxA;D function before the maintenance of AER-FGFs becomes associated with Shh signaling. Second, by studying the role of HoxA;D genes in absence of *Gli3*, which renders *Shh* functionally irrelevant.

MATERIALS AND METHODS

Mouse strains

Mutant mouse lines have been described previously: floxed *HoxA* gene cluster (Kmita et al., 2005), *HoxAnull* (Scotti and Kmita, 2012), *HoxDnull* (Spitz et al., 2001) [also referred to as $HoxD^{-}$ and named *TgHd11/lacZDel9* by Spitz et al. (Spitz et al., 2001)], *Gli3XtJ* (Hui and Joyner, 1993) and *Prx1Cre* (Logan et al., 2002). The *Shhnull* line was derived from crossing the conditional *Shh* mutant (Lewis et al., 2001) with *Mox2Cre* mice (Tallquist and Soriano, 2000). Mice and embryos were genotyped by PCR or Southern blot analysis, using genomic DNA extracted from tail biopsies and yolk sacs, respectively.

Optical projection tomography (OPT)

Optical projection tomography (OPT) microscopy (Sharpe et al., 2002) was performed according to manufacturer specifications. Briefly, stained forelimbs skeletons or buds were embedded in 1% low-melt agarose, then dehydrated in 100% methanol and cleared in a mix of Benzyl Alcohol and Benzyl Benzoate (1:2). Scanning was performed using the Bioptonics 3001M OPT Scanner (Bioptonics, UK) with SKYSCAN-3001 (Skyscan, Belgium). Three-dimensional OPT reconstructions were performed with NRecon software (Skyscan) and visualized with Bioptonics viewer (Bioptonics). Measurements were made using Imaris (Bit plane).

Whole-mount *in situ* hybridization

Whole-mount *in situ* hybridizations were performed according to standard procedures using the previously described *Shh* (Echelard et al., 1993), *Fgf8* (Crossley and Martin, 1995), *Grem1* (Zúñiga et al., 1999), *Bmp4* (Bénazet et al., 2009), *Hoxa11* and *Hoxa13* (Warot et al., 1997) antisense riboprobes.

Luciferase assay

P19 cells were transfected with 250 ng of the luciferase reporter under the control of the minimal promoter with or without enhancer sequences together with 100 ng of either Hoxd9- or Hoxa13-coding sequence or control-GFP DNA. Each plasmid combination was set in triplicates. Cell media were changed 24 hours after transfection and cells were kept in incubation for an additional 24 hours. Cell media was discarded and lysis buffer [100 mM Tris (pH 7.8), 0.5% NP-40, 1 mM DTT] was placed onto cells. Cell lysate was harvested and placed in contact with luciferin (Promega) in order to measure the reporter activity using Promega's GLOMAX 96 microplate luminometer. Fold activation was measured by comparing mean RLU values for each condition with the mean RLU value obtained for the condition determined as basal level, i.e. control luciferase reporter (no enhancer sequence) in presence of control-GFP DNA.

RESULTS

HoxA and HoxD genes are required for the initial activation of *Grem1*

Limb growth initially relies on interactions between the AER and the mesenchyme (referred to as the AER phase hereafter) until the AER regresses. Subsequently, elongation of skeletal elements defines the eventual length of the limb (referred to as the post-AER phase hereafter). We first examined whether the impact of HoxA;D function on the mesenchyme-AER interactions is mediated only by the regulation of *Shh* expression or whether it includes an independent effect of HoxA;D genes on the other factors implicated in mesenchyme-AER interactions. As HoxA;D function is required for the initial activation of *Shh* transcription, there is a narrow time window, at early bud stage, when HoxA and HoxD genes are functional, while Shh signaling is not yet operational. We thus took advantage of this Shh-independent stage to assess whether the lack of HoxA;D genes interferes with the expression of factors known to maintain AER-FGFs. Whole-mount *in situ* hybridization shows readily detectable *Grem1* expression in wild-type (Fig. 1A) and $Shh^{-/-}$ (Fig. 1B) nascent buds. *Grem1* expression is actually still detectable in $Shh^{-/-}$ buds at E10 (Fig. 1C), consistent with previous results showing that *Shh* is dispensable for the transcriptional activation of *Grem1* (Panman et al., 2006; Bénazet et al., 2009). By marked contrast, the ubiquitous deletion of the HoxA and HoxD clusters results in the complete lack of *Grem1* activation in early limb buds (Fig. 1D), indicating that the initial activation of *Grem1* requires HoxA;D function. Previous work has revealed that bone morphogenetic protein 4 (*Bmp4*) is required for the transcriptional

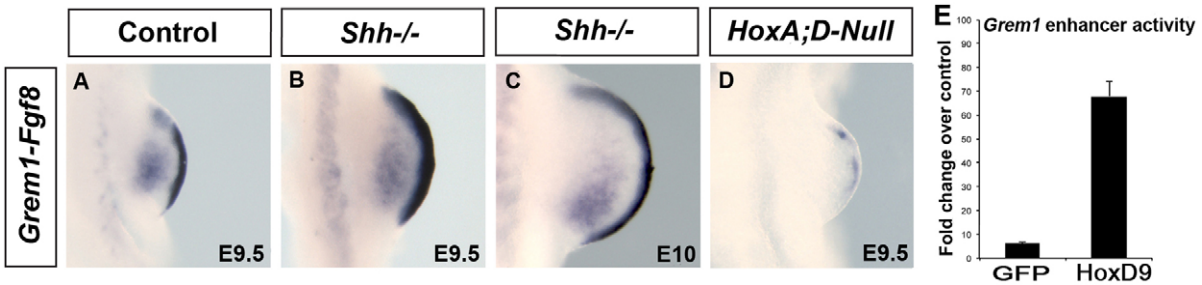

Fig. 1. HoxA;D genes are required for *Grem1* activation and a proper *Fgf8* expression pattern, independently of Shh signaling. (**A-D**) *Grem1* and *Fgf8* expression in control (A), $Shh^{-/-}$ (B,C) and *Hox(A;D)null* (D) limb buds. Although *Grem1* expression is absent in *Hox(A;D)null* bud at E9.5 (D), it is still readily detectable in E10 $Shh^{-/-}$ bud (C). (**E**) Transcription assays in P19 cells co-transfected with *Grem1* enhancer linked to luciferase-coding sequences and either the GFP or Hoxd9-expressing vector. Luciferase activity is indicated as fold change over luciferase activity in absence of the *Grem1* enhancer. Error bars represent s.d.

activation of *Grem1* in early limb buds (Bénazet et al., 2009), raising the possibility that the absence of *Grem1* expression in *Hox(A;D)null* mutants is secondary to *Bmp4* downregulation. However, *Bmp4* remains expressed in *Hox(A;D)null* limbs (supplementary material Fig. S1), thus excluding its downregulation as a cause for the lack of *Grem1* expression. In turn, these results reveal that Bmp4 signaling is unable to trigger *Grem1* activation in the absence of HoxA;D genes. To further test the competence of Hox proteins in activating *Grem1*, we next performed transcription assays in P19 cells, in which the luciferase reporter was under the control of the previously identified *Grem1* limb enhancer (Zuniga et al., 2012). In these assays, a plasmid encoding Hoxd9 was used as a representative of Hox proteins present in the nascent limb bud. Luciferase quantification reveals robust increase in the activity of the *Grem1* enhancer in presence of the Hoxd9 protein (Fig. 1E), indicating that Hoxd9 (and most likely the other early Hox genes products) is able to activate *Grem1* expression. This result, however, does not exclude the requirement of *Bmp4* together with HoxA;D genes for *Grem1* activation, as *Bmp4* is expressed in P19 cells (Chang et al., 2010).

Impaired expression of *Fgf8* in *Hox(A;D)null* nascent limb buds is coincident with *Fgf10* downregulation

Up to E10, the maintenance of *Fgf8* expression in the AER does not require *Grem1* function, as revealed by the analysis of *Grem1*-deficient limb buds (Michos et al., 2004). Consequently, the *Fgf8* downregulation observed in *Hox(A;D)null* nascent buds (Fig. 1D) suggests that another mesenchymal factor maintaining *Fgf8* expression is impaired in these mutant buds. We thus analyzed the expression of *Fgf10*, the function of which triggers *Fgf8* activation and contributes to *Fgf8* maintenance (Ohuchi et al., 1997). Our results show that *Fgf10* is downregulated anteriorly in *Hox(A;D)null* buds (Fig. 2C) compared with both wild-type (Fig. 2A) and *Shh*$^{-/-}$ buds (Fig. 2B), suggesting that HoxA;D genes contribute to *Fgf10* regulation in early buds. As *Fgf10* is initially activated in the lateral plate mesoderm, we also checked *Fgf10* expression prior to limb budding but failed to assess unambiguously whether its expression is affected or not in the presumptive limb field (not shown). In order to have an independent assessment of the capacity of Hox proteins to positively regulate *Fgf10* expression, we performed transcription assays in P19 cells. To drive expression of the luciferase reporter, we used a DNA fragment previously identified as containing the *Fgf10* limb enhancer (R2 in Fig. 2D,E) (Ohuchi et al., 2005; Sasak et al., 2002). As negative controls, we linked the reporter to the other conserved DNA fragments located upstream *Fgf10* but with no enhancer function in limbs (R1 and R3 in Fig. 2D,E), one of them acting as *Fgf10* enhancer in the inner ear [R1; see also Ohuchi et al. (Ohuchi et al., 2005)]. Upon co-transfection with the Hoxd9-encoding plasmid, there is a significant augmentation of the R2 enhancer activity, as revealed by the reporter expression, whereas the activity of R1 and R3 remained at basal levels (Fig. 2E). These results point to a specific effect of Hoxd9 protein on the activity of the enhancer controlling *Fgf10* expression in nascent buds and support the contribution of HoxA;D genes for the proper expression of *Fgf10* in the limb mesenchyme.

The anterior propagation of *Grem1* expression involves the function of HoxA;D genes

The requirement of Hox function for *Grem1* transcriptional activation raises the possibility that HoxA;D genes are also involved in *Grem1* regulation at later stages. Investigating this hypothesis

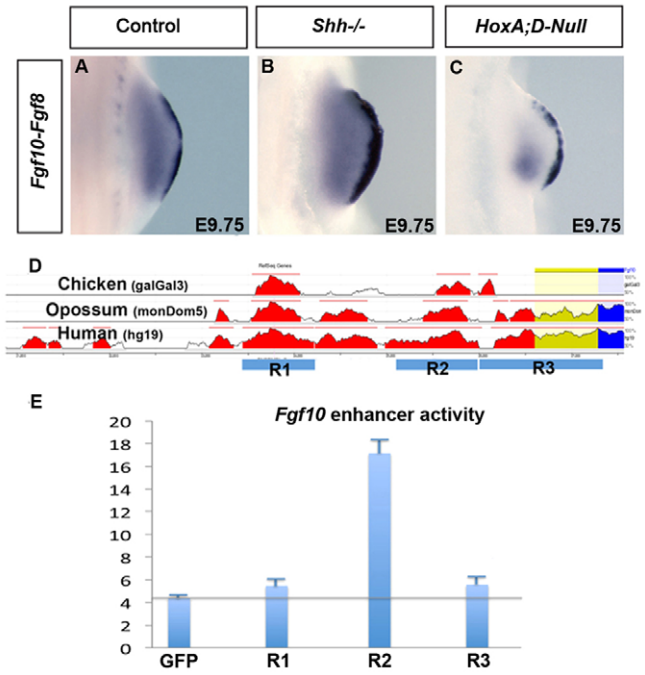

Fig. 2. *Fgf10* expression is altered in absence of HoxA;D genes. (**A-C**) *Fgf10* and *Fgf8* expression in control (A), *Shh*$^{-/-}$ (B) and *HoxA;Dnull* (C) limbs. (**D**) The genomic region upstream *Fgf10*. Three regions (R1 to R3) are conserved between mouse, chick, opossum and human. Only R2 acts as a limb enhancer. (**E**) Relative effect of Hoxd9 protein on the transcriptional activity of each conserved region. Luciferase activity is indicated as fold change over control (i.e. luciferase vector without any R regions). Error bars represent s.d.

necessitates the inactivation of HoxA;D genes after *Grem1* initial activation. This can be achieved using the *HoxAc/–;D*$^{-/-}$ conditional mutant, in which transcripts from the conditional HoxA allele are transiently generated (up to E10.5) owing to the kinetics of the *Prx1-Cre* activity (Kmita et al., 2005). Consistent with the residual HoxA transcription, *Grem1* is activated in *HoxAc/–;D*$^{-/-}$ buds (supplementary material Fig. S2). At E11.5, *Grem1* expression remains detectable in *HoxAc/–;D*$^{-/-}$ mutants, although it fails to expand anteriorly as it does in wild-type buds (Fig. 3A,B). Interestingly, *Fgf8* expression, which is normal at E10.5 (supplementary material Fig. S2C), is subsequently restricted to the part of the AER that parallels the *Grem1* domain along the AP axis (Fig. 3E, arrows), suggesting that, at this stage, *Grem1* defines the AP domain of *Fgf8* expression in the AER.

Although *Grem1* expression is posteriorly restricted in the *HoxAc/–;D*$^{-/-}$ mutant, the respective role of Hox genes and *Shh* in *Grem1* anterior expansion remains unclear because *Shh* is downregulated in *HoxAc/–;D*$^{-/-}$ limb buds (Kmita et al., 2005). To investigate the *Shh*-independent function of HoxA;D genes, we needed to remove *Gli3* function to render *Shh* functionally irrelevant (Litingtung et al., 2002; te Welscher et al., 2002). Owing to the lethality associated with *Gli3* inactivation and *HoxAc/–* mutation as well as the infertility of *HoxD*$^{-/-}$ mice, triple mutant embryos can only be generated from crosses between triple heterozygous mice. However, *HoxA*$^{+/-}$*;HoxD*$^{+/-}$*;Gli3*$^{+/-}$ turns out to be poorly fertile, which drastically reduces the feasibility of studying *HoxAc/–;HoxD*$^{-/-}$*;Gli3*$^{-/-}$ embryos. We could circumvent this limitation using the conditional *HoxA* allele instead of the null allele and we therefore performed our analysis

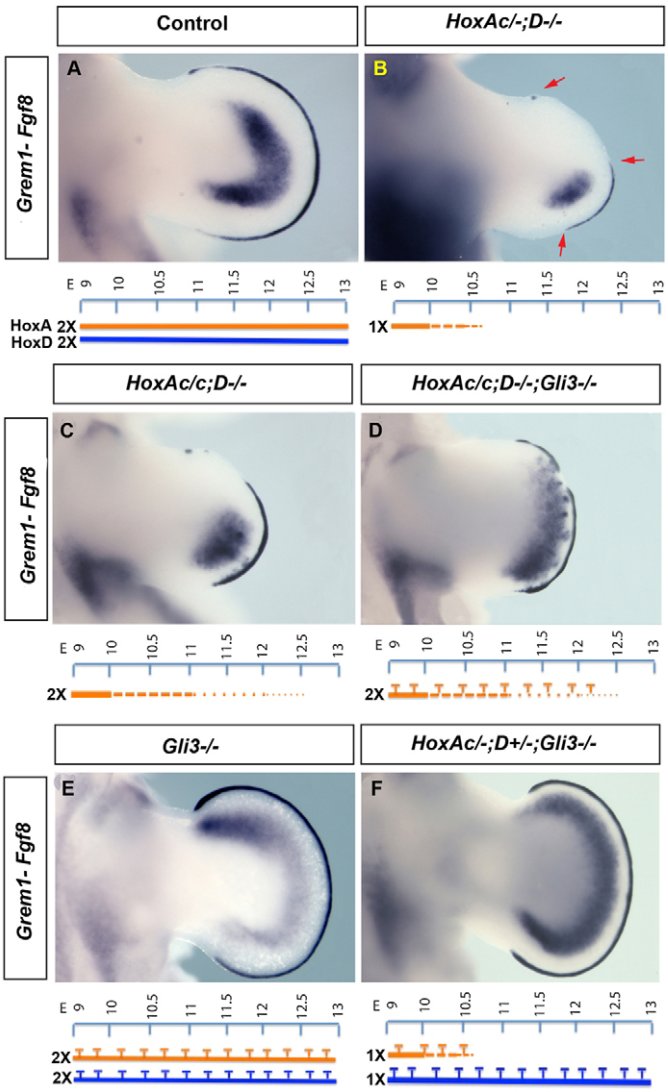

Fig. 3. *Grem1* expression is altered in the conditional *HoxA;D* mutants, even in absence of Gli3R. (**A-F**) Expression pattern of *Grem1* and *Fgf8* at E11.5 in control (A), *HoxAc/–;HoxD*$^{-/-}$ (B), *HoxAc/c;HoxD*$^{-/-}$ (C), *HoxAc/c;HoxD*$^{-/-}$*;Gli3*$^{-/-}$ (D), *Gli3*$^{-/-}$ (E) and *HoxAc/–;HoxD*$^{+/-}$*;Gli3*$^{-/-}$ (F) limb buds. Arrows in B indicate *Fgf8* expression domains. For each genotype, the *HoxA* (orange) and *HoxD* (blue) expression level and timing is schematized. Bold lines represent wild-type expression levels, whereas the Prx1Cre-dependent reduction of *HoxA* transcripts are schematized using dotted lines. T bars in D-F represent the anterior gain of Hox expression due to *Gli3* inactivation. The presence of two HoxA conditional alleles (*HoxAc/c*) results in more HoxA expression when one of the two alleles is null (supplementary material Fig. S3), leading to more *Grem1* expression (compare B with C). The patchy expression pattern of *Grem1* in *HoxAc/c;HoxD*$^{-/-}$ (C), *HoxAc/c;HoxD*$^{-/-}$*;Gli3*$^{-/-}$ (D) coincides with the mosaic expression of *Hoxa13* (see also supplementary material Fig. S5).

with triple mutants in which both *HoxA* alleles are conditional (*HoxAc/c;HoxD*$^{-/-}$*;Gli3*$^{-/-}$), which were obtained at the expected Mendelian ratio (1/128). The difference between *HoxAc/c* and *HoxAc/–* is that the completion of Cre-mediated deletion is delayed with two floxed alleles and some *HoxA* expression remains at least up to E11.5 (supplementary material Fig. S3). Comparison of *HoxAc/c;HoxD*$^{-/-}$*;Gli3*$^{-/-}$ with *HoxAc/c;HoxD*$^{-/-}$ buds, at E11.5, reveals an anteriorization of both *Grem1* and *Fgf8* in the triple mutant (Fig. 3C-D). However, expression of both genes remains clearly impaired compared with *Gli3*$^{-/-}$ and *Shh*$^{-/-}$*;Gli3*$^{-/-}$ mutant (Fig. 3E) (see also Litingtung et al., 2002; te Welscher et al., 2002). Notably, in *HoxAc/c;HoxD*$^{-/-}$*;Gli3*$^{-/-}$ buds, *Grem1* expression is mosaic and significantly reduced in the anterior mesenchyme (Fig. 3D compared with 3E). This indicates that *Gli3* inactivation is not sufficient to restore the anterior expansion of *Grem1* in *HoxAc/c;HoxD*$^{-/-}$*;Gli3*$^{-/-}$ as it does in *Shh*$^{-/-}$*;Gli3*$^{-/-}$ buds and raises the possibility that HoxA;D genes contribute to this process.

We reasoned that if Hox proteins contribute to *Grem1* anterior expansion, *Grem1* expression in *HoxAc/c;HoxD*$^{-/-}$*;Gli3*$^{-/-}$ should be, at least in part, due to the residual transcription of the conditional HoxA allele, notably that of *Hoxa13,* which is the most distally expressed HoxA gene. Accordingly, the gain of *Grem1* upon *Gli3* inactivation (Fig. 3D) coincides with the anterior expansion of the residual *Hoxa13* expression (supplementary material Fig. S4B), which itself is due to the lack of the Gli3R repressor. *Grem1* expansion could also be secondary to the lack of Gli3R. However, the correlation between the mosaicism of *Grem1* expression and that of the residual *Hoxa13* expression observed in *HoxAc/c;HoxD*$^{-/-}$ and *HoxAc/c;HoxD*$^{-/-}$*;Gli3*$^{-/-}$ (Fig. 3C,D; supplementary material Fig. S5) strongly favors the interpretation that HoxA;D genes are required for the proper anterior expansion of *Grem1*. Accordingly, a single wild-type allele of the HoxA or HoxD cluster is sufficient to recover the anterior *Grem1* expression as in *Gli3*$^{-/-}$ and *Shh*$^{-/-}$*;Gli3*$^{-/-}$ (shown for the HoxD wild-type allele in Fig. 3F, compare with 3D and 3E).

To test independently the effect of the Hoxa13 protein on *Grem1* expression, we performed a transcription assay in P19 cells. Co-transfection of the expression vector encoding for Hoxa13 together with the *Grem1* limb enhancer linked to the luciferase reporter resulted in a significantly higher reporter expression, as revealed by luciferase quantification (supplementary material Fig. S6), confirming that Hoxa13 has a positive impact on the activity of the *Grem1* limb enhancer. Together, these results provide evidence that HoxA;D genes contribute to the anterior expansion of *Grem1* expression independently of their function in controlling *Shh*.

The AP and PD growth in the *Gli3*$^{-/-}$ background involves the function of HoxA;D genes

Our data on *Grem1* expression support the notion that HoxA;D genes promote limb bud growth in parallel to their function in regulating *Shh.* In turn, it suggests that limb bud growth should vary according to the HoxA;D dose, independently of *Shh* expression. We thus performed measurements of limb buds using optical projection tomography (OPT) imaging to characterize how reducing the HoxA;D gene dose in the *Gli3*$^{-/-}$ background affects limb bud growth. At E11.5, reduction of the Hox dose to a single HoxA or HoxD wild-type allele results in the shortening of the limb bud along the PD axis (Fig. 4A,B). In addition, this shortening is more pronounced upon further reduction of the HoxA;D dose (Fig. 4C,D). These data reveal a tight link between the HoxA;D dose and the extent of PD bud growth in the *Gli3* mutant background. Our series of *HoxA;D;Gli3* mutants also show that one functional allele of either *HoxA* or *HoxD* is sufficient to generate the distal 'fan-shaped' characteristic of *Gli3*$^{-/-}$ limb bud (Fig. 4A,B) but this shape is lost with lower Hox doses (Fig. 4C,D). This suggests that the AP expansion of the distal bud observed in *Gli3*$^{-/-}$ and *Shh*$^{-/-}$*;Gli3*$^{-/-}$ buds is associated with the function of HoxA;D genes.

Together, our series of *HoxA;D;Gli3* mutants reveals a link between the HoxA;D dose and the extent of PD and AP bud growth in the *Gli3*$^{-/-}$ background.

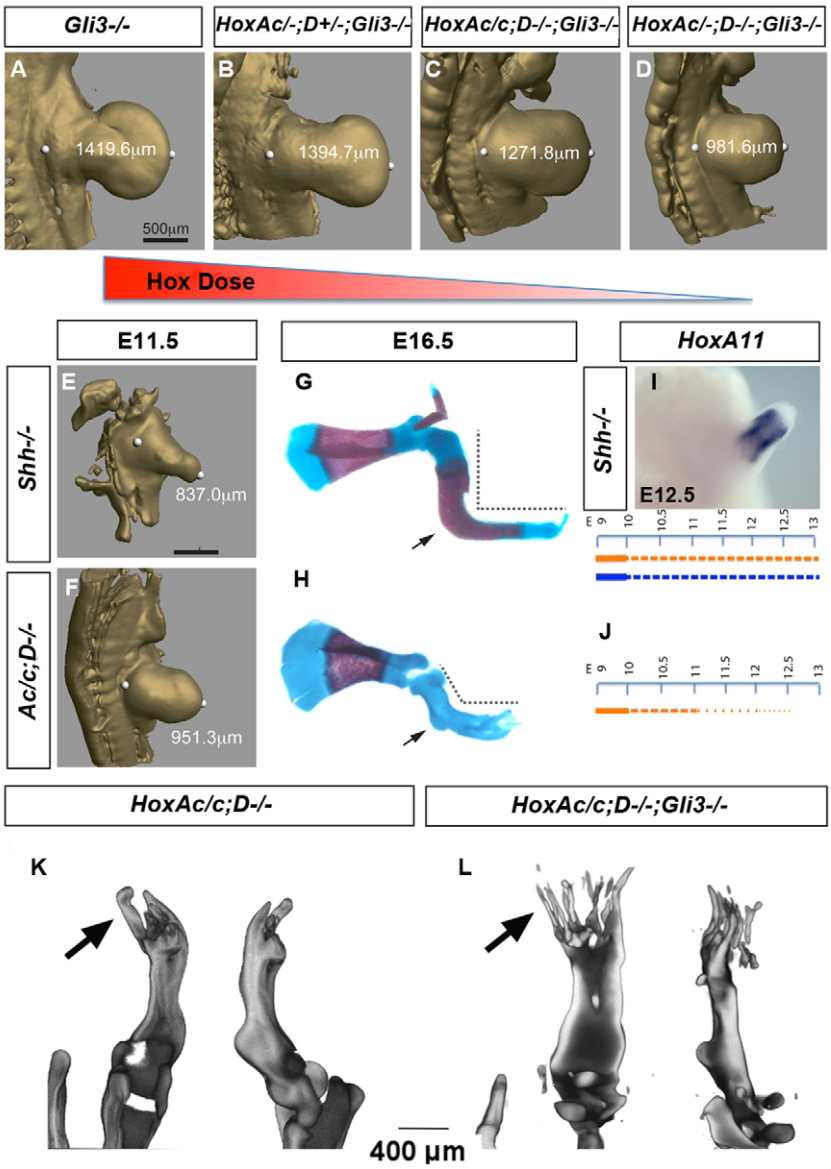

Fig. 4. Reduction of the HoxA;D dose in the *Gli3* mutant background results in the gradual decrease of limb bud size. (**A-D**) OPT imaging and measurements of limb buds from *Gli3*$^{-/-}$ (A), *HoxAc/–;HoxD*$^{+/-}$*;Gli3*$^{-/-}$ (B), *HoxAc/c;HoxD*$^{-/-}$*;Gli3*$^{-/-}$ (C) and *HoxAc/–;HoxD*$^{-/-}$*;Gli3*$^{-/-}$ (D) mutants. Measurements were made from the distal tip of the limb bud to the 'groove-type' shape at the proximal end of the bud (dot). (**E**,**F**) OPT imaging and measurements of *Shh*$^{-/-}$ (E) and *HoxAc/c;HoxD*$^{-/-}$ (F) limb buds at E11.5. (**G**,**H**) Forelimb skeleton of *Shh*$^{-/-}$ (G) and *HoxAc/c;HoxD*$^{-/-}$ (H) mutants at E16.5. Arrows indicate the similar bending observed in these mutant skeletons. (**I**,**J**) *Hoxa11* expression at E12.5 in *Shh*$^{-/-}$ forelimb buds and schemes representing the persistence at late stages of HoxA;D expression in *Shh* mutant (I) in contrast to the transient expression of the conditional HoxA allele in the *HoxAc/c;HoxD*$^{-/-}$ mutant (J). (**K**,**L**) OPT imaging of *HoxAc/c;HoxD*$^{-/-}$ (K) and *HoxAc/c;HoxD*$^{-/-}$*;Gli3*$^{-/-}$ (L) forelimb skeletons at E16.5. Ventral view is on the left part of each panel and lateral view is on the right. Arrows indicate similar banding in *Shh*$^{-/-}$ and *HoxAc/c;* and *D*$^{-/-}$ skeleton.

HoxA;D downregulation and the defective growth of *Shh*$^{-/-}$ limb

In absence of *Shh*, the domain of Gli3R, which is normally restricted to the most anterior part of the limb bud, expands towards the posterior part (Wang et al., 2000). This results in the downregulation of several genes in most of the *Shh*$^{-/-}$ limb bud, including HoxA;D genes (Chiang et al., 2001; Kraus et al., 2001). The rescue of the *Shh*$^{-/-}$ limb phenotype upon removal of *Gli3* indicates that the downregulation of the direct and/or indirect targets of Gli3R is responsible for the *Shh*$^{-/-}$ phenotype. Our finding that the HoxA;D gene dose in the *Gli3*$^{-/-}$ background correlates with limb bud growth thus suggests that *Shh*$^{-/-}$ limb truncation is, at least in part, the consequence of Gli3R-mediated HoxA;D downregulation. Nonetheless, as *Shh* remains transiently expressed in the conditional *HoxA;D* mutant (Kmita et al., 2005), there is less Gli3R-mediated gene repression, including less repression of the residual *HoxA* expression, than in the *Shh* mutant and thus it is possible that *HoxAc/c;HoxD*$^{-/-}$ buds could develop better than *Shh*$^{-/-}$ buds until complete *HoxA* inactivation. In agreement with this view, at E11.5, *Shh*$^{-/-}$ buds are smaller than *HoxAc/c;HoxD*$^{-/-}$ buds (Fig. 4E,F).

The size difference between *Shh*$^{-/-}$ and the conditional *HoxA;D* buds is opposite when skeletons are compared (Fig. 4G,H), indicating that the elongation of the skeletal elements is favored in *Shh* mutant. Interestingly, around E12, there is a complete deficiency of Hox expression in *HoxAc/c;HoxD–/–* buds, while Hox expression persists in *Shh* mutant (Fig. 4I-J). Actually *HoxA11* expression in *Shh* mutant appears even stronger at E12.5 than at E11.5 (Fig. 4I; supplementary material Fig. S7). This sustained *Hox* expression in *Shh*$^{-/-}$ (Fig. 4I) could explain the favored elongation of skeletal elements, consistent with previous reports proposing that the elongation of skeletal elements requires the function of HoxA;D genes (Boulet and Capecchi, 2004; Gross et al., 2012; Zákány et al., 1997). In *Shh*$^{-/-}$*;Gli3*$^{-/-}$ limb, proper elongation of skeletal elements is thus expected to be associated with HoxA;D function. Yet it remains unclear whether other Gli3R targets are implicated. To clarify this issue, we compared the skeleton of the conditional *HoxA;D* and *HoxA;D;Gli3* limbs and found that they are similarly shorten along the PD axis (Fig. 4K-L). This result indicates that among Gli3R targets, HoxA;D genes have the most relevant role for the elongation of skeletal elements.

Transient expression of the conditional HoxA allele allows for the realization of a rudimentary but complete PD axis

The *HoxAc/c;HoxD*$^{-/-}$*;Gli3*$^{-/-}$ skeleton at E16.5 is characterized by the increased number of distal rays when compared with *HoxAc/c;HoxD*$^{-/-}$ skeletons (Fig. 4K,L). This increased number of distal rays is reminiscent of the increased number of digits in *Gli3*$^{-/-}$ limbs, thus raising the possibility that these distal rays correspond to digit remnants. However, the lack of digit-specific features, such as segmentation into distinct phalanges, makes it difficult to assign an identity unambiguously to these rays. Interestingly, *HoxAc/+;HoxD*$^{-/-}$ and *HoxAc/c;HoxD*$^{+/-}$ limbs, although being significantly smaller than wild-type ones, have the three domains (stylopod, zeugopod and autopod), allowing for unambiguous identification of digits despite their abnormal shape and absence of segmentation into phalanges (Fig. 5A,C). Moreover, the comparison with *HoxAc/+;HoxD*$^{-/-}$*;Gli3*$^{-/-}$ and with *HoxAc/c;HoxD*$^{+/-}$*;Gli3*$^{-/-}$ limbs (Fig. 5B,D) shows that *Gli3* inactivation in these Hox mutant backgrounds primarily affects the number of digital condensations. Together, these data support our interpretation that the distal rays in *HoxAc/c;HoxD*$^{-/-}$*;Gli3*$^{-/-}$ limbs are digit remnants.

Interestingly, the bending systematically found in the middle of *HoxAc/c;HoxD*$^{-/-}$ skeletons (arrow in Fig. 4H) evokes the bending of wild-type limbs at the transition between stylopod and zeugopod (Fig. 5E). Remarkably, *Shh* mutant embryos form either a clearly distinct stylopod and zeugopod separated by a rudimentary elbow joint (e.g. Litingtung et al., 2002) or limbs with only the bend typically associated with the elbow joint (arrow in Fig. 4G) (see also Zhu et al., 2008), supporting that the bending observed in *HoxAc/c;HoxD*$^{-/-}$ mutant limbs corresponds to a vestige of the stylopod-zeugopod boundary. Thus, the phenotype of *HoxAc/c;HoxD*$^{-/-}$ and *HoxAc/c;HoxD*$^{-/-}$*;Gli3*$^{-/-}$ skeletons suggests that the transient expression of HoxA genes is sufficient to provide cells with a stylopod, zeugopod or digit identity depending of which HoxA genes they express.

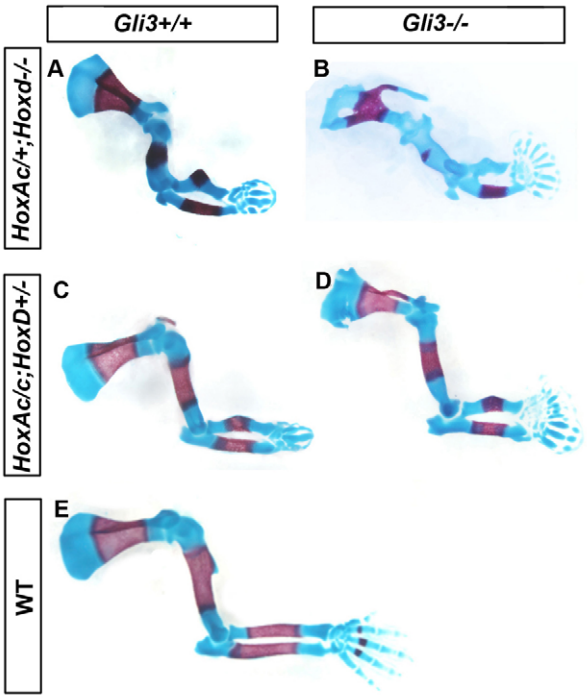

Fig. 5. *Gli3* inactivation does not improve the elongation of skeletal elements of mutant with reduced dose of *HoxA;D* genes but triggers the formation of additional digits. (**A-D**) E16.5 forelimb skeletal preparations from *HoxAc/+;HoxD*$^{-/-}$ (A,B) and *HoxAc/c;HoxD*$^{+/-}$ (C,D) in the presence (A,C) or absence (B,D) of *Gli3* . (**E**) Wild-type forelimb skeleton at E16.5. A single functional copy of the HoxD (C,D) or HoxA (A,B) cluster is sufficient for the formation of the three limb domains, but the reduced Hox dose interferes with the elongation of each domain. In the absence of *Gli3* (B,D), PD length is not improved but there is a significant increase in digit number.

DISCUSSION

During limb development, genes of the HoxA and HoxD clusters are expressed in a spatial and temporal co-linear manner. Genetics studies previously established the role of Hox genes in limb skeletal patterning but their role in limb bud growth remains unclear, mainly owing to the crossregulation existing between HoxA;D genes and *Shh*. The work reported here provides a novel perspective on the role of Hox genes in limb bud growth and the mechanisms involved. First, we show that in nascent bud, prior to the normal activation of *Shh*, the function of HoxA;D genes is required for correct *Fgf8* expression. Moreover, we establish that HoxA;D genes achieve this previously unrecognized role through the transcriptional activation of *Grem1* and proper expression of *Fgf10* in the mesenchyme. Second, taking advantage of *Gli3* inactivation that renders *Shh* expression functionally irrelevant, we provide evidence that the anterior expansion of *Grem1* expression, and thus the propagation of Grem1-mediated maintenance of AER-FGFs, requires the function of HoxA;D genes independently of their activity in regulating *Shh* expression. Accordingly, our data show that during the Shh functional phase, the proper AP and PD growth of the limb bud requires the Shh-independent functions of HoxA;D genes. Finally, we also show that HoxA;D genes are subsequently required for the elongation of skeletal elements.

Multiple inputs of Hox genes on the epithelial-mesenchymal interactions triggering limb bud growth

Limb bud growth first relies on epithelial-mesenchymal (EM) interactions that trigger and then maintain expression of AER-FGFs, up to AER regression around E13. The initial EM interaction, which induces limb budding, relies on Fgf10 signaling from the lateral plate mesoderm (LPM) that triggers expression of *Fgf8* in the overlaying ectoderm (Ohuchi et al., 1997). Activation of *Fgf10* expression in the presumptive forelimb field of the LPM relies on Tbx5 (Agarwal et al., 2003; Rallis et al., 2003). Recently, analysis of *Tbx5* regulation identified Hox proteins from paralogous group 4 and 5 as regulators of *Tbx5* expression in the LPM (Minguillon et al., 2012). Despite the absence of *Hoxd4*, *Hoxa4* and *Hoxa5* in the LPM of *Hox(A;D)null* embryos, we did not detect clear modification of *Fgf10* expression in the LPM (not shown), suggesting that the absence of HoxA;D genes in the LPM has minor, if any, impact on the Tbx5-mediated regulation of *Fgf10*. Therefore, the effect of the *Hox(A;D)null* mutation on *Fgf10* expression is primarily associated with the function of HoxA;D genes in the developing limb bud, consistent with the evidence that Hoxd9 protein positively influence the activity of the *Fgf10* early limb enhancer in cell culture assays. The evidence that *Fgf10* expression is not abrogated in *Hox(A;D)null* limb bud but only reduced suggests that *Fgf10* regulation involves HoxA;D proteins, as well as other transcription factors. Interestingly, switching expression of *Hoxd12* and *Hoxd13* from late to early bud stages in absence of *Gli3* suppresses *Fgf10* expression in the limb mesenchyme (Zakany et al., 2007). It was thus proposed that *Fgf10* downregulation is the

consequence of the functional suppression of early expressed Hox by 'late'-activated Hox genes (Zakany et al., 2007), which supports the model that Hox genes expressed in early limb buds act as positive regulators of *Fgf10*. Together, these results point to the implication of Hox genes in the early EM interactions, first through the impact of both group 4 and 5 Hox genes on *Fgf10* expression in the LPM and second through the function of *HoxA;D* genes in the nascent limb bud.

Although *Grem1* is activated in nascent bud, its function in maintaining *Fgf8* in the AER becomes indispensable around E10, as revealed by the analysis of the *Grem1* mutant (Michos et al., 2004). *Grem1* downregulation in *Shh* mutant and the ability of Shh-soaked beads implanted in the anterior mesenchyme to trigger ectopic *Grem1* expression provided evidence that Shh signaling acts positively on *Grem1* expression (Zúñiga et al., 1999). However, Shh signaling is not needed for the initial activation of *Grem1* in nascent bud (Panman et al., 2006; Bénazet et al., 2009). Moreover, inactivating *Shh* together with its direct intracellular mediator Gli3 prevents *Grem1* downregulation (Litingtung et al., 2002; te Welscher et al., 2002), indicating that *Grem1* downregulation in *Shh* mutant is due to Gli3R activity, although Gli3 repression of *Grem1* has been proposed to be indirect (Vokes et al., 2008). As Gli3R also leads to HoxA;D downregulation, it is possible that Gli3R repression of *Grem1* is secondary to Hox repression. Our results strongly support this interpretation: first, in contrast to *Shh*, HoxA;D function is required for the initial activation of *Grem1* in nascent bud. Second, *Gli3* inactivation in the conditional *HoxA;D* mutant background is not sufficient to restore *Grem1* expression, as reported for the $Shh^{-/-};Gli3^{-/-}$ mutant. Finally, the mosaicism of *Grem1* in the conditional *HoxA;D;Gli3* mutant strongly correlates with the mosaicism of the residual HoxA gene expression in this mutant.

Based on this previously unappreciated function of *HoxA;D* genes in eliciting *Grem1* expression, which occurs independently of their role in regulating *Shh* expression, we propose a novel model for the control of *Grem1* expression (Fig. 6). In this model, *HoxA;D* genes trigger the initial activation of *Grem1* (either in cooperation or in parallel with Bmp4 signaling) in nascent limb bud. Concomitantly, they activate *Shh* expression in the ZPA. In turn, Shh signaling restricts Gli3 proteolytic cleavage into a transcriptional repressor to the most anterior mesenchymal cells, thereby defining a domain permissive for the expression of *HoxA;D* genes and subsequent propagation of *Grem1* expression.

HoxA;D genes and the control of limb bud growth

By uncoupling Hox and *Shh* functions using *Gli3* inactivation, which renders Shh functionally irrelevant, we now provide evidence that Hox genes control bud growth in parallel to their activity in controlling *Shh* expression. Notably, we found that during the AER phase, reducing the *HoxA;D* gene dose in absence of *Gli3* interferes with limb bud growth in a dose-dependent manner, both along the AP and PD axes. Previous studies suggesting that the elongation of skeletal elements requires HoxA;D function were based on ubiquitous gene inactivation (Boulet and Capecchi, 2004; Gross et al., 2012; Zákány et al., 1997). Our data suggest that at least part of the reported phenotype could have been due to defective growth during the AER phase. Nonetheless, the comparison between the size of $Shh^{-/-}$ and the conditional *HoxA;D* mutant at E11.5 and E16.5 further supports the requirement of Hox products for the elongation of the skeletal elements at the post-AER stages. Moreover, the difference in *Fgf8* expression in the conditional *HoxA;D* and *HoxA;D;Gli3* mutants (and thus the difference in the size of the pool of skeletal precursors) has no detectable effect on the eventual size of the skeleton along the PD axis, further highlighting the importance of HoxA;D function in the elongation of skeletal elements.

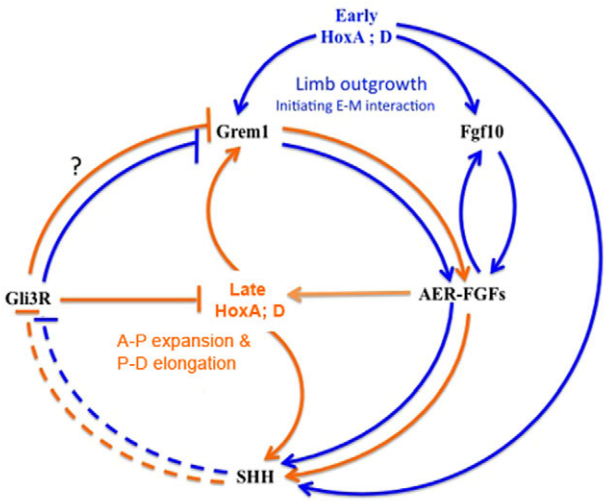

Fig. 6. Model for the sequential inputs of HoxA;D genes on the maintenance of AER-FGFs. In nascent limb buds (blue lines), early activated HoxA;D genes trigger the initial activation of *Grem1* (either in cooperation or in parallel with Bmp4 signaling) and *Shh*, and contribute to the proper expression of *Fgf10* in nascent buds. At this stage, *Fgf10* function is sufficient to ensure *Fgf8* expression in the AER. By the time Shh signaling is activated, it restricts (dashed lines) Gli3 proteolytic cleavage into a transcriptional repressor to the most anterior mesenchymal cells, thereby defining a domain permissive for the expression of HoxA;D genes. Later activated HoxA;D genes (orange) maintain *Shh* expression and associated anterior restriction of Gli3R. In parallel, they contribute to the anterior expansion of *Grem1*, which is required for proper FGF expression in the anterior AER and AP expansion of the distal bud (presumptive autopod). All interactions represent transcriptional inputs except the one indicated by broken lines, which is a post-translational effect.

Together, these results provide compelling evidence for a Hox-dependent *Shh*-independent mechanism that promotes limb bud growth during the AER phase, as well as the requirement of *HoxA;D* genes for the subsequent elongation of skeletal elements.

Hox-FGF crossregulation

Exhaustive analysis of the function of AER-FGFs suggested that AER-FGF signaling contributes to PD patterning in addition to limb bud growth (Mariani et al., 2008). Interestingly, recent work provided evidence that AER-FGF signaling has a key role for the expression of 'late/distal' Hox genes (i.e. group 11 to 13), as revealed by the Fgf8 requirement for the sequential activation of *Hoxa11* and *Hoxa13* in limb mesenchymal cells in culture (Cooper et al., 2011; Roselló-Díez et al., 2011) and *Hoxd13* downregulation associated with a reduced dose of AER-FGFs (Sun et al., 2002). These genes actually instruct cells of their PD identity (zeugopod identity for *Hox11* and autopod identity for *Hox13*) and thereby likely represent the effectors through which AER-FGFs influence PD patterning. Our finding that early activated HoxA;D genes promote the maintenance of AER-FGFs suggests that, in addition to providing proximal identity to cells where they are expressed, early activated HoxA;D genes ensure proper AER-FGF-dependent expression of late/distal HoxA;D genes. Accordingly, the Hox-FGF-positive cross-regulation would control limb bud growth and ensure some steadiness between the formation of proximal and distal identity.

Conclusions

In summary, our data uncover a previously unappreciated role of HoxA;D genes in the control of AER-FGFs expression, which provides a novel perspective on the role of HoxA;D genes in limb growth (Fig. 6). First, in nascent limb buds, early-activated HoxA and HoxD genes contribute to the proper expression of *Fgf10* and as a consequence proper *Fgf8* expression in the AER. Concomitantly, Hox proteins are required to activate *Grem1* and *Shh* and set up the cross-regulation between Shh, Gli3 and HoxA;D genes as well as the Grem1-dependent maintenance of AER-FGFs. In turn, AER-FGF signaling subsequently triggers the sequential activation of 'late' HoxA and HoxD genes, which specify intermediate (zeugopod) and distal (autopod) identity and are essential to sustain growth along both P-D and A-P axis. In parallel, Shh signaling, by restricting the processing of the Gli3 protein into a transcriptional repressor to anterior limb mesenchymal cells, maintains the A-P biased expression of HoxD genes that subsequently translates into A-P patterning. The dual role of HoxA;D genes in controlling growth pathways and patterning, from early limb bud stages onwards, establishes a molecular link between these two processes, which need to be precisely coordinated to ensure robustness of the limb architecture.

Acknowledgements

We are thankful to Aurélie de Ronne, Jessica Barthe and Marisa Junco for technical help, and to Pierre Chambon, Denis Duboule and Rolf Zeller for providing mutant lines. We are particularly grateful to Rolf Zeller and Cliff Tabin for insightful comments on our data.

Funding

This work was supported by the Canadian Institute of Health Research [CIHR-82880 to M.K.], the Canada Research Chairs program (to M.K.) and the Spanish Ministry of Science and Innovation [BFU2011-24972 to M.A.R.]. R.S. was supported by the Angelo Pizzagalli post-doctoral fellowship, D.G. was supported by a post-doctoral fellowship from the Fonds de la Recherche en Santé du Québec and M.S. was supported by a pre-doctoral fellowship from the Molecular Biology program of the University of Montreal.

Competing interests statement

The authors declare no competing financial interests.

Supplementary material

Supplementary material available online at
http://dev.biologists.org/lookup/suppl/doi:10.1242/dev.089409/-/DC1

References

Agarwal, P., Wylie, J. N., Galceran, J., Arkhitko, O., Li, C., Deng, C., Grosschedl, R. and Bruneau, B. G. (2003). Tbx5 is essential for forelimb bud initiation following patterning of the limb field in the mouse embryo. *Development* **130**, 623-633.

Bénazet, J. D., Bischofberger, M., Tiecke, E., Gonçalves, A., Martin, J. F., Zuniga, A., Naef, F. and Zeller, R. (2009). A self-regulatory system of interlinked signaling feedback loops controls mouse limb patterning. *Science* **323**, 1050-1053.

Boulet, A. M. and Capecchi, M. R. (2004). Multiple roles of Hoxa11 and Hoxd11 in the formation of the mammalian forelimb zeugopod. *Development* **131**, 299-309.

Boulet, A. M., Moon, A. M., Arenkiel, B. R. and Capecchi, M. R. (2004). The roles of Fgf4 and Fgf8 in limb bud initiation and outgrowth. *Dev. Biol.* **273**, 361-372.

Capellini, T. D., Di Giacomo, G., Salsi, V., Brendolan, A., Ferretti, E., Srivastava, D., Zappavigna, V. and Selleri, L. (2006). Pbx1/Pbx2 requirement for distal limb patterning is mediated by the hierarchical control of Hox gene spatial distribution and Shh expression. *Development* **133**, 2263-2273.

Chang, G., Miao, Y. L., Zhang, Y., Liu, S., Kou, Z., Ding, J., Chen, D. Y., Sun, Q. Y. and Gao, S. (2010). Linking incomplete reprogramming to the improved pluripotency of murine embryonal carcinoma cell-derived pluripotent stem cells. *PLoS ONE* **5**, e10320.

Chiang, C., Litingtung, Y., Harris, M. P., Simandl, B. K., Li, Y., Beachy, P. A. and Fallon, J. F. (2001). Manifestation of the limb prepattern: limb development in the absence of sonic hedgehog function. *Dev. Biol.* **236**, 421-435.

Cooper, K. L., Hu, J. K., ten Berge, D., Fernandez-Teran, M., Ros, M. A. and Tabin, C. J. (2011). Initiation of proximal-distal patterning in the vertebrate limb by signals and growth. *Science* **332**, 1083-1086.

Crossley, P. H. and Martin, G. R. (1995). The mouse Fgf8 gene encodes a family of polypeptides and is expressed in regions that direct outgrowth and patterning in the developing embryo. *Development* **121**, 439-451.

Duboule, D. and Morata, G. (1994). Colinearity and functional hierarchy among genes of the homeotic complexes. *Trends Genet.* **10**, 358-364.

Echelard, Y., Epstein, D. J., St-Jacques, B., Shen, L., Mohler, J., McMahon, J. A. and McMahon, A. P. (1993). Sonic hedgehog, a member of a family of putative signaling molecules, is implicated in the regulation of CNS polarity. *Cell* **75**, 1417-1430.

Fallon, J. F., López, A., Ros, M. A., Savage, M. P., Olwin, B. B. and Simandl, B. K. (1994). FGF-2: apical ectodermal ridge growth signal for chick limb development. *Science* **264**, 104-107.

Galli, A., Robay, D., Osterwalder, M., Bao, X., Bénazet, J. D., Tariq, M., Paro, R., Mackem, S. and Zeller, R. (2010). Distinct roles of Hand2 in initiating polarity and posterior Shh expression during the onset of mouse limb bud development. *PLoS Genet.* **6**, e1000901.

Gross, S., Krause, Y., Wuelling, M. and Vortkamp, A. (2012). Hoxa11 and Hoxd11 regulate chondrocyte differentiation upstream of Runx2 and Shox2 in mice. *PLoS ONE* **7**, e43553.

Hui, C. C. and Joyner, A. L. (1993). A mouse model of greig cephalopolysyndactyly syndrome: the extra-toesJ mutation contains an intragenic deletion of the Gli3 gene. *Nat. Genet.* **3**, 241-246.

Kmita, M., Tarchini, B., Zàkàny, J., Logan, M., Tabin, C. J. and Duboule, D. (2005). Early developmental arrest of mammalian limbs lacking HoxA/HoxD gene function. *Nature* **435**, 1113-1116.

Knezevic, V., De Santo, R., Schughart, K., Huffstadt, U., Chiang, C., Mahon, K. A. and Mackem, S. (1997). Hoxd-12 differentially affects preaxial and postaxial chondrogenic branches in the limb and regulates Sonic hedgehog in a positive feedback loop. *Development* **124**, 4523-4536.

Kraus, P., Fraidenraich, D. and Loomis, C. A. (2001). Some distal limb structures develop in mice lacking Sonic hedgehog signaling. *Mech. Dev.* **100**, 45-58.

Laufer, E., Nelson, C. E., Johnson, R. L., Morgan, B. A. and Tabin, C. (1994). Sonic hedgehog and Fgf-4 act through a signaling cascade and feedback loop to integrate growth and patterning of the developing limb bud. *Cell* **79**, 993-1003.

Lewis, P. M., Dunn, M. P., McMahon, J. A., Logan, M., Martin, J. F., St-Jacques, B. and McMahon, A. P. (2001). Cholesterol modification of sonic hedgehog is required for long-range signaling activity and effective modulation of signaling by Ptc1. *Cell* **105**, 599-612.

Litingtung, Y., Dahn, R. D., Li, Y., Fallon, J. F. and Chiang, C. (2002). Shh and Gli3 are dispensable for limb skeleton formation but regulate digit number and identity. *Nature* **418**, 979-983.

Logan, M., Martin, J. F., Nagy, A., Lobe, C., Olson, E. N. and Tabin, C. J. (2002). Expression of Cre Recombinase in the developing mouse limb bud driven by a Prxl enhancer. *Genesis* **33**, 77-80.

Mariani, F. V., Ahn, C. P. and Martin, G. R. (2008). Genetic evidence that FGFs have an instructive role in limb proximal-distal patterning. *Nature* **453**, 401-405.

Michos, O., Panman, L., Vintersten, K., Beier, K., Zeller, R. and Zuniga, A. (2004). Gremlin-mediated BMP antagonism induces the epithelial-mesenchymal feedback signaling controlling metanephric kidney and limb organogenesis. *Development* **131**, 3401-3410.

Minguillon, C., Nishimoto, S., Wood, S., Vendrell, E., Gibson-Brown, J. J. and Logan, M. P. (2012). Hox genes regulate the onset of Tbx5 expression in the forelimb. *Development* **139**, 3180-3188.

Moon, A. M., Boulet, A. M. and Capecchi, M. R. (2000). Normal limb development in conditional mutants of Fgf4. *Development* **127**, 989-996.

Niswander, L. and Martin, G. R. (1993). FGF-4 and BMP-2 have opposite effects on limb growth. *Nature* **361**, 68-71.

Ohuchi, H., Nakagawa, T., Yamamoto, A., Araga, A., Ohata, T., Ishimaru, Y., Yoshioka, H., Kuwana, T., Nohno, T., Yamasaki, M. et al. (1997). The mesenchymal factor, FGF10, initiates and maintains the outgrowth of the chick limb bud through interaction with FGF8, an apical ectodermal factor. *Development* **124**, 2235-2244.

Ohuchi, H., Yasue, A., Ono, K., Sasaoka, S., Tomonari, S., Takagi, A., Itakura, M., Moriyama, K., Noji, S. and Nohno, T. (2005). Identification of cis-element regulating expression of the mouse Fgf10 gene during inner ear development. *Dev. Dyn.* **233**, 177-187.

Panman, L., Galli, A., Lagarde, N., Michos, O., Soete, G., Zuniga, A. and Zeller, R. (2006). Differential regulation of gene expression in the digit forming area of the mouse limb bud by SHH and gremlin 1/FGF-mediated epithelial-mesenchymal signalling. *Development* **133**, 3419-3428.

Rallis, C., Bruneau, B. G., Del Buono, J., Seidman, C. E., Seidman, J. G., Nissim, S., Tabin, C. J. and Logan, M. P. (2003). Tbx5 is required for forelimb bud formation and continued outgrowth. *Development* **130**, 2741-2751.

Roselló-Díez, A., Ros, M. A. and Torres, M. (2011). Diffusible signals, not autonomous mechanisms, determine the main proximodistal limb subdivision. *Science* **332**, 1086-1088.
Sasak, H., Yamaoka, T., Ohuchi, H., Yasue, A., Nohno, T., Kawano, H., Kato, S., Itakura, M., Nagayama, M. and Noji, S. (2002). Identification of cis-elements regulating expression of Fgf10 during limb development. *Int. J. Dev. Biol.* **46**, 963-967.
Scotti, M. and Kmita, M. (2012). Recruitment of 5′ Hoxa genes in the allantois is essential for proper extra-embryonic function in placental mammals. *Development* **139**, 731-739.
Sharpe, J., Ahlgren, U., Perry, P., Hill, B., Ross, A., Hecksher-Sørensen, J., Baldock, R. and Davidson, D. (2002). Optical projection tomography as a tool for 3D microscopy and gene expression studies. *Science* **296**, 541-545.
Spitz, F., Gonzalez, F., Peichel, C., Vogt, T. F., Duboule, D. and Zákány, J. (2001). Large scale transgenic and cluster deletion analysis of the HoxD complex separate an ancestral regulatory module from evolutionary innovations. *Genes Dev.* **15**, 2209-2214.
Sun, X., Lewandoski, M., Meyers, E. N., Liu, Y. H., Maxson, R. E., Jr and Martin, G. R. (2000). Conditional inactivation of Fgf4 reveals complexity of signalling during limb bud development. *Nat. Genet.* **25**, 83-86.
Sun, X., Mariani, F. V. and Martin, G. R. (2002). Functions of FGF signalling from the apical ectodermal ridge in limb development. *Nature* **418**, 501-508.
Tallquist, M. D. and Soriano, P. (2000). Epiblast-restricted Cre expression in MORE mice: a tool to distinguish embryonic vs. extra-embryonic gene function. *Genesis* **26**, 113-115.
Tarchini, B., Duboule, D. and Kmita, M. (2006). Regulatory constraints in the evolution of the tetrapod limb anterior-posterior polarity. *Nature* **443**, 985-988.
te Welscher, P., Zuniga, A., Kuijper, S., Drenth, T., Goedemans, H. J., Meijlink, F. and Zeller, R. (2002). Progression of vertebrate limb development through SHH-mediated counteraction of GLI3. *Science* **298**, 827-830.
Vokes, S. A., Ji, H., Wong, W. H. and McMahon, A. P. (2008). A genome-scale analysis of the cis-regulatory circuitry underlying sonic hedgehog-mediated patterning of the mammalian limb. *Genes Dev.* **22**, 2651-2663.
Wang, B., Fallon, J. F. and Beachy, P. A. (2000). Hedgehog-regulated processing of Gli3 produces an anterior/posterior repressor gradient in the developing vertebrate limb. *Cell* **100**, 423-434.
Warot, X., Fromental-Ramain, C., Fraulob, V., Chambon, P. and Dollé, P. (1997). Gene dosage-dependent effects of the Hoxa-13 and Hoxd-13 mutations on morphogenesis of the terminal parts of the digestive and urogenital tracts. *Development* **124**, 4781-4791.
Xu, B. and Wellik, D. M. (2011). Axial Hox9 activity establishes the posterior field in the developing forelimb. *Proc. Natl. Acad. Sci. USA* **108**, 4888-4891.
Zakany, J. and Duboule, D. (2007). The role of Hox genes during vertebrate limb development. *Curr. Opin. Genet. Dev.* **17**, 359-366.
Zákány, J., Fromental-Ramain, C., Warot, X. and Duboule, D. (1997). Regulation of number and size of digits by posterior Hox genes: a dose-dependent mechanism with potential evolutionary implications. *Proc. Natl. Acad. Sci. USA* **94**, 13695-13700.
Zákány, J., Kmita, M. and Duboule, D. (2004). A dual role for Hox genes in limb anterior-posterior asymmetry. *Science* **304**, 1669-1672.
Zakany, J., Zacchetti, G. and Duboule, D. (2007). Interactions between HOXD and Gli3 genes control the limb apical ectodermal ridge via Fgf10. *Dev. Biol.* **306**, 883-893.
Zeller, R., López-Ríos, J. and Zuniga, A. (2009). Vertebrate limb bud development: moving towards integrative analysis of organogenesis. *Nat. Rev. Genet.* **10**, 845-858.
Zhu, J., Nakamura, E., Nguyen, M. T., Bao, X., Akiyama, H. and Mackem, S. (2008). Uncoupling Sonic hedgehog control of pattern and expansion of the developing limb bud. *Dev. Cell* **14**, 624-632.
Zúñiga, A., Haramis, A. P., McMahon, A. P. and Zeller, R. (1999). Signal relay by BMP antagonism controls the SHH/FGF4 feedback loop in vertebrate limb buds. *Nature* **401**, 598-602.
Zuniga, A., Laurent, F., Lopez-Rios, J., Klasen, C., Matt, N. and Zeller, R. (2012). Conserved cis-regulatory regions in a large genomic landscape control SHH and BMP-regulated Gremlin1 expression in mouse limb buds. *BMC Dev. Biol.* **12**, 23.